Journal of Biomolecular NMR, **23:** 211–219, 2002.
KLUWER/ESCOM

Determination of residual dipolar couplings in homonuclear MOCCA-SIAM experiments

Andreas Möglich[a], Michael Wenzler[a], Frank Kramer[b], Steffen J. Glaser[b] & Eike Brunner[a,*]
[a]*University of Regensburg, Institute of Biophysics and Physical Biochemistry, D-93040 Regensburg, Germany;*
[b]*Technical University of Munich, Institute of Organic Chemistry and Biochemistry II, D-85747 Garching, Germany*

Received 12 April 2002; Accepted 1 May 2002

Key words: MOCCA mixing sequence, NMR, protein structure, residual dipolar couplings, SIAM experiment

Abstract

In solutions with partial molecular alignment, anisotropic magnetic interactions such as the chemical shift anisotropy, the electric quadrupole interaction, and the magnetic dipole-dipole interaction are no longer averaged out to zero in contrast to isotropic solutions. The resulting residual anisotropic magnetic interactions are increasingly used in biological NMR studies for the determination of 3D structures of proteins and other biomolecules. In the present paper we propose a new approach allowing the measurement of residual H^N-H^α dipolar couplings of non-isotope enriched proteins based on the application of the MOCCA-SIAM experiment. This experiment allows the measurement of homonuclear coupling constants with an accuracy of ca. ± 0.2 Hz and is therefore particularly well suited to determine residual dipolar couplings at relatively low degrees of molecular orientation. The agreement between experimentally determined residual H^N-H^α couplings and calculated values is demonstrated for BPTI.

Abbreviations: 2D, two-dimensional; 3D, three-dimensional; ACME, amplitude-constrained multiplet evaluation; BPTI, basic pancreatic trypsin inhibitor; COSY, correlation spectroscopy; CTAB, hexadecyl(cetyl)trimethylammonium bromide; DHPC, dihexanoylphosphatidylcholine; DMPC, dimyristoylphosphatidylcholine; DQF, double-quantum filtered; EDTA, ethylenediaminetetraacetic acid; FID, free induction decay; MOCCA, modified phase-cycled Carr-Purcell; NMR, nuclear magnetic resonance; NOE, nuclear Overhauser effect; RMSD, root mean square deviation; TOCSY, total correlation spectroscopy; TPPI, time-proportional phase incrementation; SIAM, simultaneous acquisition of in-phase and anti-phase multiplets; ZQF, zero-quantum filtered.

Introduction

Residual dipolar couplings between two nuclei, 1 and 2, occur if molecules in solution exhibit a partial molecular orientation. Their magnitude is given by Equation 1 (Bastiaan et al., 1987).

$$\langle D_{12} \rangle = -D_{12}^{\text{stat}} S_{zz} S \left\{ \left(\frac{3}{2} \cos^2 \vartheta - \frac{1}{2} \right) + \frac{\eta}{2} \sin^2 \vartheta \cos 2\varphi \right\}. \quad (1)$$

The angles ϑ and φ are the polar angles defining the orientation of the internuclear vector relative to the principal axis system of the so-called molecular alignment tensor which is described by an order matrix, S_{ij}. The principal values of this matrix are denoted by S_{xx}, S_{yy}, and S_{zz}, where $|S_{zz}| \geq |S_{yy}| \geq |S_{xx}|$. The asymmetry parameter, η, is defined as $\eta = (S_{xx} - S_{yy})/S_{zz}$. The so-called static dipolar coupling constant, D_{12}^{stat}, is given by Equation 2.

$$D_{12}^{\text{stat}} = \frac{\mu_0 \gamma_1 \gamma_2 h}{8\pi^3 \langle r_{12}^3 \rangle}, \quad (2)$$

h is the Planck constant and μ_0 the permeability of vacuum. γ_1 and γ_2 denote the gyromagnetic ratios of the spins 1 and 2. The distance between spins 1 and 2 has to be averaged in the presence of dis-

*To whom correspondence should be addressed. E-mail: eike.brunner@biologie.uni-regensburg.de

tance variations such as vibrations. This is indicated by the brackets in Equation 2. The order parameter S ($0 \leq S \leq 1$) in Equation 1 accounts for the influence of local internal molecular motions different from the reorientation of the entire molecule.

In addition to NOE data, residual dipolar couplings provide valuable information for the NMR spectroscopic structure determination of biomolecules (see, e.g., Tjandra and Bax, 1997; Clore et al., 1999; Fowler et al., 2000; Mueller et al., 2000; Brunner, 2001; Bax et al., 2001). Residual dipolar couplings are nowadays widely used for structure refinement. They are capable of replacing NOE data to a very high extent (Clore et al., 1999). Moreover, an increasing number of attempts is made to determine protein structures mainly on the basis of residual dipolar couplings (Fowler et al., 2000; Annila et al., 1999; Delaglio et al., 2000; Meiler et al., 2000; Simon et al., 2002).

Residual dipolar couplings containing relevant structural information are observed, e.g., in heteronuclear spin systems such as ^{1}H-^{15}N or ^{1}H-^{13}C pairs. Apart from these frequently used heteronuclear one-bond couplings, residual dipolar couplings also occur in homonuclear ^{1}H-^{1}H spin systems, such as H^N-H^α pairs. The effect of residual dipolar couplings upon homonuclear two-dimensional (2D) NMR correlation spectra (COSY, Jeener, 1971; Aue et al., 1976) of oligosaccharides and nucleic acids has been demonstrated by Bolon and Prestegard (1998), Hansen et al. (1998a,b). Several approaches have been described to measure residual H^N-H^α dipolar couplings in proteins using double- and triple-resonance experiments. Prestegard and coworkers described the use of the constant-time COSY method (Tian et al., 2000) and Cai et al. (1999) have used a non-proton decoupled HNCA experiment. Peti and Griesinger (2000) suggested the J_{HH}-NOESY experiment which is based on the E. COSY principle (Griesinger et al., 1985). Tjandra and Bax (1997) employed the HNHA experiment (Vuister and Bax, 1993) to observe residual H^N-H^α dipolar couplings. Otting et al. (2000) described the use of a modified J_{HH}-TOCSY experiment (Willker and Leibfritz, 1992).

For some systems such as, e.g., the muscle proteins actin and myosin, however, isotope enriched samples are not available yet. Previously, we have demonstrated that the 2D COSY experiment can be used to determine residual dipolar couplings of non-isotope enriched samples (Brunner et al., 2000). Residual dipolar couplings, $\langle D_{12} \rangle$, between two J-coupled spins such as intraresidue H^N-H^α pairs are added to the isotropic coupling constant, J_{12}, resulting in an effective coupling constant, $J_{eff} = J_{12} + \langle D_{12} \rangle$ (Bastiaan et al., 1987). Note that both, J_{12} and $\langle D_{12} \rangle$ may be positive or negative. For intraresidue H^N-H^α pairs, $J_{12} = {}^3J_{HNH\alpha}$ is positive and falls within the range between 4 and 10 Hz. The residual dipolar couplings can, therefore, easily be determined as the difference between the effective coupling constants measured in anisotropic and isotropic solution provided that the sign of J_{eff} is known. Since the 2D COSY experiment does not allow to determine the sign of J_{eff}, it is necessary to fulfill the condition$|J_{12}| > |\langle D_{12} \rangle|$. That means, relatively low degrees of molecular alignment have to be chosen. However, the precise measurement of small residual dipolar couplings of the order of 1–3 Hz in ordinary 2D COSY experiments is often impossible. The previously described ACME program allows to determine homonuclear ^{1}H-^{1}H coupling constants from 2D COSY experiments with an improved accuracy ($\pm$0.5 Hz; Delaglio et al., 2001).

In this contribution we describe the use of a TOCSY-based homonuclear 2D NMR experiment, the so-called MOCCA-SIAM experiment (Prasch et al., 1998) offering an enhanced accuracy compared to common 2D COSY experiments.

Materials and methods

As shown in Figure 1, the SIAM experiment (Prasch et al., 1998) was employed with a MOCCA-XY16 mixing sequence (Kramer et al., 2001) which is optimized for dipolar transfer. In the SIAM experiment, two separate FIDs are recorded per t_1-increment (FID1 and FID2). Addition of FID1 and FID2 yields an in-phase spectrum (ZQF-SIAM) whereas subtraction produces an anti-phase spectrum (DQF-SIAM).

The NMR samples contained 2.0 mM BPTI and 0.1 mM EDTA in 50 mM potassium phosphate buffer at pH = 6.2. Partial molecular orientation of the protein was achieved by adding a bicelle-forming mixture of phospholipids which contained DMPC, DHPC, and CTAB in a molar ratio of 3:1:0.1 (Ottiger and Bax, 1998; Losonczi and Prestegard, 1998). The anisotropic solution additionally contained 4 wt-% of the above-mentioned mixture of phospholipids. All spectra were recorded on a Bruker DMX-500 spectrometer (^{1}H-frequency of 500.13 MHz) at 305.0 K. The mixing time for the MOCCA-XY16 sequence was 25 ms to ensure efficient transfer. The length of the π mixing pulse was $d = 40$ μs and the pulse delay was

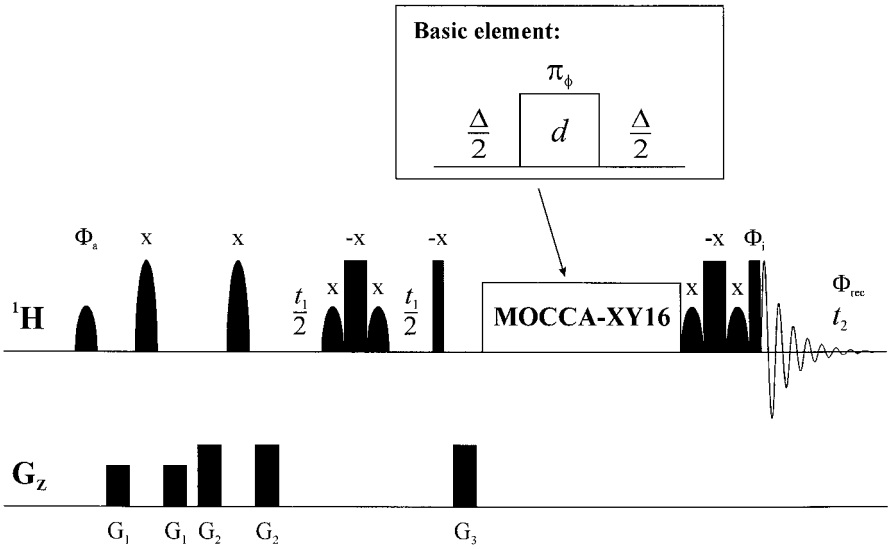

Figure 1. Pulse sequence of the MOCCA-XY16-SIAM experiment. Narrow bars: 'Hard' 90° pulses, wide bars: 'Hard' 180° pulses, small bell-shaped symbols: 90° shaped pulses selective for the H^α region (Q5 pulses (Emsley and Bodenhausen, 1992) with a duration of 4.5 ms), large bell-shaped symbols: 180° shaped pulses selective for the H^α region (Q3 pulses with a duration of 1.8 ms). The phase Φ_a was incremented using TPPI (Marion and Wüthrich, 1983), phase cycles of the last 90° pulse and the receiver were Φ_i: x, −x for FID1 and y, −y for FID2; Φ_{rec}: x, −x for FID1 and y, −y for FID2. A XY-16 supercycle was employed for the MOCCA mixing sequence Φ = x, y, x, y, y, x, y, x, −x, −y, −x, −y, −y, −x, −y, −x (Gullion et al., 1990; Lizak et al., 1991). G_1-G_3 are gradients of 1 ms duration which remove undesired magnetization. Relative gradient strengths are $G_3 = G_2 = 1.5\ G_1$.

$\Delta = 88$ μs. Per t_1-increment, 48 scans were recorded (24 for FID1 and 24 for FID2). The digital resolution of the spectra in t_2-direction was 0.2 Hz.

Due to the fact that both, an in-phase and an anti-phase spectrum are detected, values for coupling constants could be determined not only by fitting the traces of the cross-peaks to Lorentzian lineshapes as in 2D COSY experiments. A much higher accuracy is obtained by using the so-called Titman–Keeler procedure (Titman and Keeler, 1990). To determine the active coupling constant, J_{active}, of a cross-peak, traces of the cross-peak in the in-phase and anti-phase spectrum were taken and convoluted with an anti-phase and an in-phase stick doublet of separation J_{trial}, respectively. After correcting for different baseline offset and amplitude factors in the two spectra, the RMSD between the two curves was determined and normalized to the average peak intensity. The coupling constant, J_{active}, is given by that J_{trial} yielding the minimum RMSD value. Note that the Titman-Keeler procedure does not make any assumptions about the lineshape of the cross-peaks. The only condition to be fulfilled is that the lineshapes of the in-phase and the anti-phase doublet components of a given cross-peak are identical. This condition turns out to be fulfilled since (i) the in-phase and anti-phase spectra are obtained simultaneously and (ii) the doublet components have identical relaxation rates during t_2 in the zero-quantum filtered and the double-quantum filtered spectrum.

Results and discussion

MOCCA-SIAM experiments were carried out on BPTI in isotropic as well as in anisotropic solution. A contour plot of the ZQF-SIAM and the DQF-SIAM spectra of BPTI in anisotropic solution is shown in Figure 2. The values of the coupling constants were determined by using the Titman-Keeler procedure (see Table 1). The use of this procedure is demonstrated in Figure 3 for the H^N-H^α cross-peak of the residue isoleucine 18 of BPTI. J_{trial} was incremented in steps of 0.2 Hz. The plot of the normalized RMSD versus J_{trial} (see Figure 3) shows a well-defined minimum for J_{trial} corresponding to the 'true' coupling constant, J_{active}. Although the minimum of the curve shown in Figure 3 can be determined with a much higher precision, the experimental error for the thus determined coupling constant is estimated not to exceed a maximum error of ±0.2 Hz. In order to check the precision of this method, we compared the coupling constants measured in isotropic solution with the values previously published for BPTI (Pardi et al., 1984).

Table 1. Coupling constants determined in isotropic and anisotropic solution as well as residual dipolar couplings measured and calculated for BPTI. Only those amino acid residues for which the H^N-H^α-coupling constant could be measured at least in isotropic solution are listed. For comparison, the coupling constants determined by Pardi et al. (1984) are also shown. The last column of the table indicates whether a residue is located within a well-defined secondary structure element or not. Only residues within canonical secondary structure elements have been used for the determination of the molecular alignment tensor and for the calculation of the correlation and quality factors

Residue	J_{Pardi}/Hz	J_{iso}/Hz	J_{aniso}/Hz	$\langle D_{12}\rangle$/Hz	Calc. $\langle D_{12}\rangle$/Hz	2°
Asp-3	3.8	3.5	–	–	–	no
Cys-5	4.9	4.8	5.3	0.5	0.8	yes
Leu-6	8.1	8.4	9.6	1.2	1.3	yes
Tyr-10	10.1	9.8	8.3	−1.5	−0.2	no
Lys-15	8.7	8.7	9.4	0.7	0.9	no
Ala-16	7.4	8.0	8.5	0.5	1.9	no
Arg-17	9.3	9.4	8.6	−0.8	−0.7	yes
Ile-18	9.2	8.8	10.4	1.6	1.4	yes
Ile-19	6.9	6.8	6.4	−0.4	−0.2	yes
Tyr-21	10.2	9.7	10.2	0.5	0.3	yes
Phe-22	9.1	9.0	10.6	1.6	1.8	yes
Tyr-23	6.7	7.3	7.2	−0.1	0.1	yes
Asn-24	8.7	9.4	10.4	1.0	1.1	yes
Ala-25	3.9	3.2	–	–	–	no
Lys-26	6.1	6.2	4.8	−1.4	−1.9	no
Ala-27	7.8	8.0	8.6	0.6	0.8	no
Leu-29	7.0	7.5	8.8	1.3	1.0	yes
Cys-30	9.1	8.9	8.2	−0.7	−0.3	yes
Gln-31	10.2	9.5	–	–	–	yes
Thr-32	8.1	8.0	8.5	0.5	0.6	yes
Phe-33	7.1	7.4	7.1	−0.3	0.3	yes
Val-34	8.8	8.4	8.4	0.0	0.3	yes
Arg-39	6.9	7.2	7.1	−0.1	0.3	no
Lys-41	10.2	10.2	10.2	0.0	0.7	no
Asn-43	7.4	7.6	7.9	0.3	0.4	no
Asn-44	7.9	7.8	7.3	−0.5	−0.3	no
Phe-45	10.0	10.2	11.0	0.8	0.6	yes
Lys-46	6.1	5.8	5.7	−0.1	−1.1	no
Ser-47	8.3	8.2	10.0	1.8	1.8	yes
Glu-49	4.3	3.6	–	–	–	yes
Asp-50	4.9	4.4	4.8	0.4	0.6	yes
Met-52	5.2	4.4	–	–	–	yes
Arg-53	4.1	4.2	–	–	–	yes
Thr-54	6.5	6.6	7.7	1.1	1.0	yes
Cys-55	9.4	9.2	10.1	0.9	1.0	yes
Ala-58	5.7	6.2	6.8	0.6	–[a]	no

[a]The X-ray structure does not exhibit atomic coordinates for this residue due to the absence of electronic density.

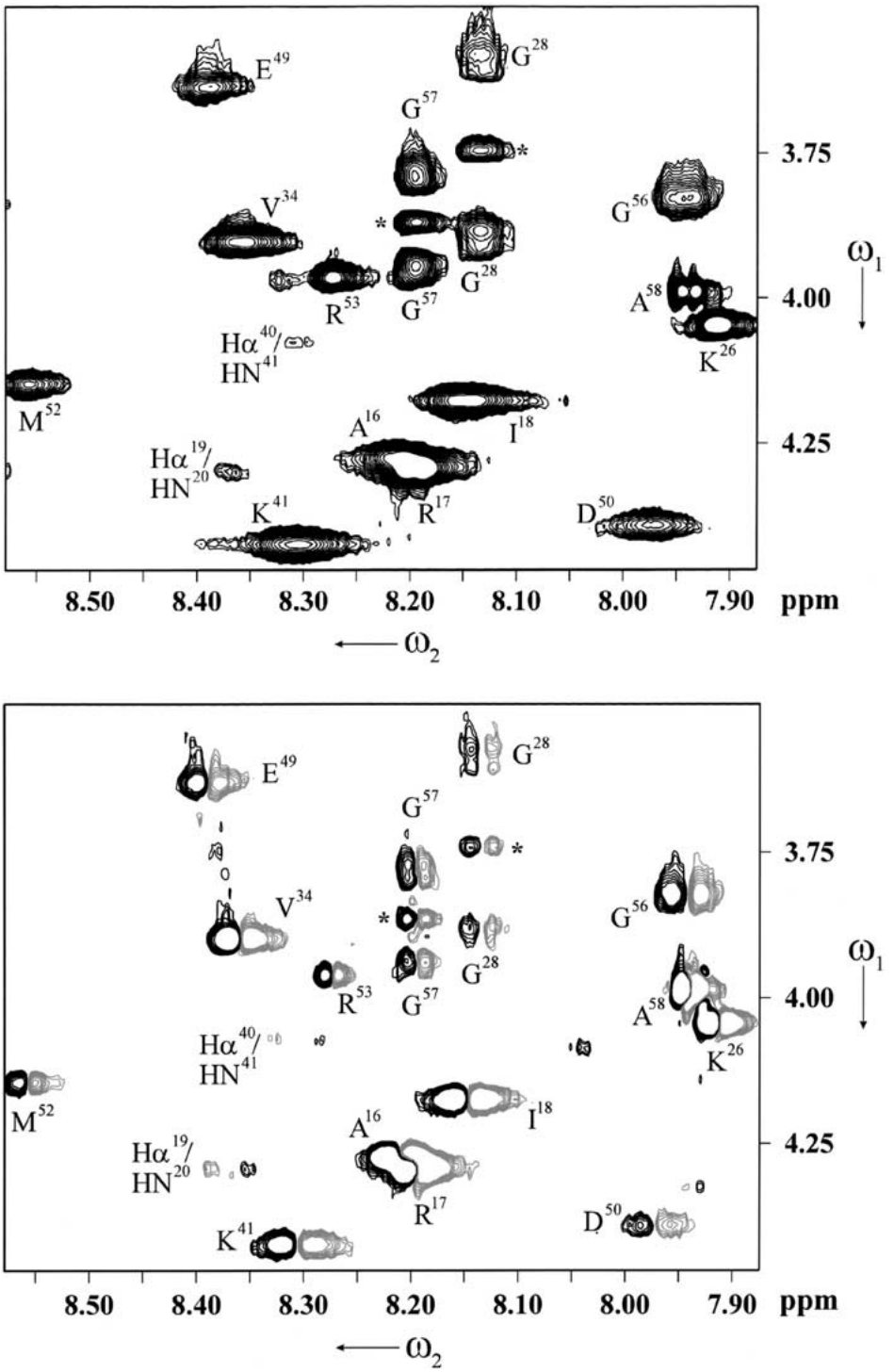

Figure 2. Top: ZQF-SIAM and bottom: DQF-SIAM. Spectra were recorded on a Bruker DMX-500 spectrometer (^{1}H-frequency of 500.13 MHz) at 305.0 K. Solution conditions were 2.0 mM BPTI, 0.1 mM EDTA, 50 mM potassium phosphate buffer at pH = 6.2, and 4 wt-% DHPC/DMPC/CTAB (see text). Note the existence of purely dipolarly coupled cross-peaks (see for example the cross-peak between H^{α} of I19 and H^{N} of R20). The appearance of an additional cross-peak for glycine residues with non-degenerate H^{α} protons at the average resonance frequency of the two H^{α} protons (see asterisks in the spectra) should also be noted. As shown in Appendix A, these signals are due to the use of shaped pulses having a duration of the order of milliseconds.

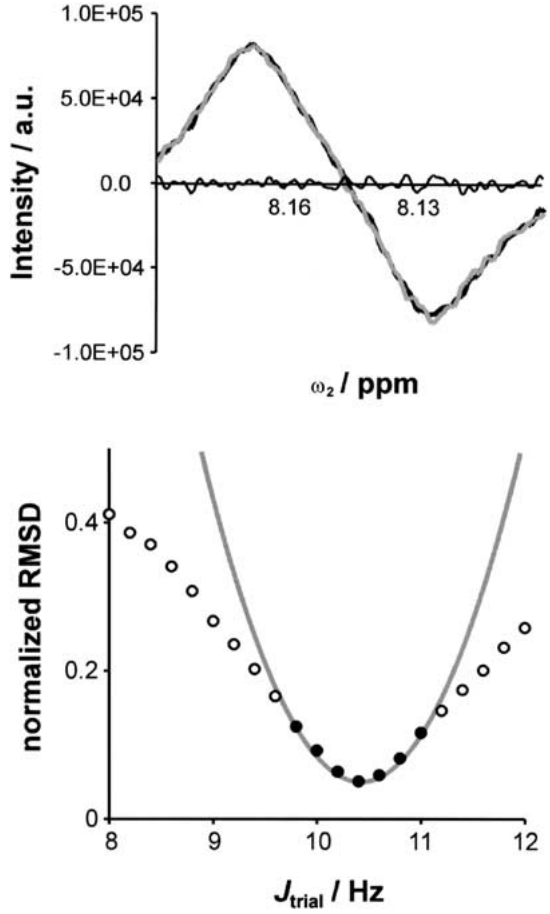

Figure 3. Top: H^N-H^α cross-peak of I18 in anisotropic solution and demonstration of the Titman–Keeler procedure used to determine the coupling constants. The trace of the cross-peak in the in-phase spectrum was convoluted with an anti-phase stick doublet of $J_{\text{trial}} = 10.4$ Hz (bold black line). Correspondingly, the trace from the anti-phase spectrum was convoluted with an in-phase doublet of identical J_{trial} (bold gray line). The thin black line shows the difference between the two curves. Bottom: Normalized RMSD between convoluted in-phase and anti-phase traces as a function of J_{trial} (circles). The bold gray line shows the fit of a second order polynomial curve $Y = aX^2 + bX + c$ to the filled circles close to the mimum (a = 0.189, b = −3.935, and c = 20.562). A well-defined minimum can be seen at 10.4 Hz.

Although the temperature and the solution conditions were different in the two studies the coupling constants were found to be in excellent agreement. A plot of our data against the values determined by Pardi et al. (1984) yields a linear correlation of slope 1 with a correlation coefficient of 0.981.

The residual dipolar couplings were determined as the difference between the coupling constants measured in anisotropic solution and the values obtained in isotropic solution. With both these measurements having a maximum experimental error of ±0.2 Hz, the maximum experimental error for the residual dipolar couplings is ±0.4 Hz.

The protein BPTI consists of 58 amino acid residues, four of which are prolines not possessing an amide proton. Six are glycine residues which were excluded from the analysis since the measurement of residual dipolar couplings is complicated by the presence of two H^α-protons. We were able to measure residual dipolar couplings for approximately 2/3 of the remaining residues (for 30 residues, see Table 1). A major improvement is the opportunity to conduct experiments at relatively low degrees of orientation due to the small experimental error of this method. In our previous 2D COSY experiments (Brunner et al., 2000) we were not able to measure negative residual dipolar couplings. The larger experimental errors in common COSY experiments necessarily require a higher degree of molecular orientation. Therefore, negative residual dipolar couplings usually lead to the complete suppression of the corresponding cross-peaks due to mutual cancellation of the anti-phase doublet components. In contrast, the application of the MOCCA-SIAM experiment also allows to measure negative residual dipolar couplings; a further advantage.

In order to assess the quality of the measured data, residual dipolar couplings were calculated for the previously determined X-ray structure of BPTI (Wlodawer et al., 1987; PDB-entry 6PTI). Using this structure and our measured residual dipolar couplings we were able to determine the molecular alignment tensor by using the computer programs SVD (Losonczi et al., 1999) and DipoCoup (Meiler et al., 2000). It is known that internal motions in proteins lead to a decrease of the order parameter S and, therefore, to reduced residual dipolar couplings for spin pairs located in the flexible regions of the molecules (see Equation 1). In addition, highly mobile regions are often not very well-defined both in NMR and X-ray structures. For these reasons, only the 19 residual dipolar couplings of amino acid residues located in well-defined canonical secondary structure elements of the molecule were taken into account. Both computer programs which were used for the determination of the molecular alignment tensor gave equivalent results. Cornilescu et al. (1998) suggested to use a so-called quality factor, defined as the normalized RMSD between experimentally determined and calculated values of the residual dipolar couplings in order to evaluate the quality of a structure. This quality factor should not exceed 0.3

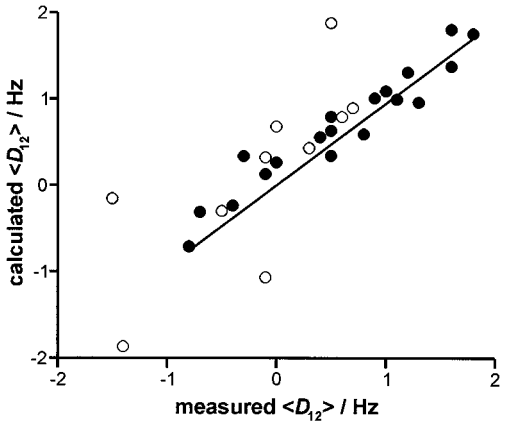

Figure 4. Correlation between experimentally determined and calculated residual dipolar couplings. For the calculation of the molecular alignment tensor and of the correlation coefficient only amino acid residues located in well-defined secondary structure elements were considered (filled circles). The correlation coefficient amounts to 0.960. Open circles show residual dipolar couplings of residues located outside of canonical secondary structure elements.

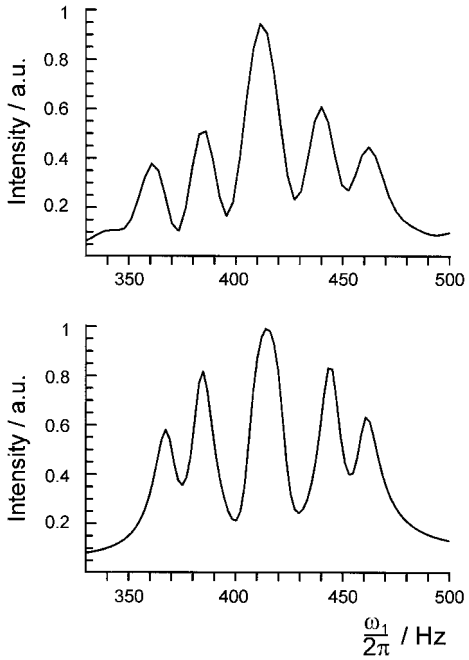

Figure 5. Top: ω_1-trace of the experimental 2D spectrum at $\omega_2 = 2\pi\nu(H^N)$ of G57. Bottom: Simulated ω_1-trace of G57 based on the effective Hamiltonian of Equation A2 for the band-selective inversion element.

for protein structures of sufficient quality. We obtained a quality factor of 0.259 which shows that the residual dipolar couplings could be determined reasonably well. The correlation between experimentally determined and calculated residual dipolar couplings is shown in Figure 4. A correlation coefficient of 0.960 was obtained taking into account only residues located in canonical secondary structure elements (filled circles in Figure 4). It is interesting to note that the absolute values of residual dipolar couplings measured for amino acid residues located outside of secondary structure elements often tend to be smaller than the calculated values (open circles in Figure 4). This is in agreement with the prediction of Equation 1 because the order parameter S describing internal motions, which amounts to ca. 0.9 in well-defined secondary structure elements (Kay et al., 1989), may become much smaller in flexible regions of the molecules.

In summary, it can be stated that the MOCCA-XY16-SIAM experiment facilitates precise measurements of residual H^N-H^α dipolar couplings of non-isotope enriched samples. Compared to the previously described 2D COSY experiments, this new approach provided enhanced precision, i.e., a maximum experimental error of only ± 0.4 Hz for the residual dipolar couplings. The reduced experimental error in SIAM experiments allows to measure residual dipolar couplings at low degrees of molecular orientation. This allows to fulfill the condition $|J_{12}| > |\langle D_{12} \rangle|$ even for $J_{12} = {}^3J_{HNH\alpha}$ in H^N-H^α pairs, i.e., it is possible to measure negative residual dipolar couplings also in homonuclear experiments of non-isotope enriched samples.

The H^N-H^α coupling constants measured in isotropic solution also provide valuable information about the conformation of the protein backbone (Karplus, 1959). The superb precision of the isotropic coupling constants is therefore an additional advantage of the use of the MOCCA-SIAM experiment for protein structure determination. Another advantage of the described approach is the opportunity to use different TOCSY mixing sequences.

Acknowledgements

The authors wish to thank Prof Dr Hans Robert Kalbitzer for numerous helpful discussions. Financial support by the Deutsche Forschungsgemeinschaft is gratefully acknowledged by M.W. (SFB 521, project No. 910025), S.J.G. (project Gl 203/1-6), and E.B. (projects Br 1278/8-2 and 1278/9-1). F.K. and S.J.G. highly appreciate grants awarded by the Fonds der chemischen Industrie.

Appendix A

In glycine ^{1}H spin systems, consisting of H^N, H^α, and $H^{\alpha'}$, only two cross-peaks are expected in the H^N-H^α region of the SIAM experiment. For example, at $\omega_2 = 2\pi\nu(H^N)$, cross-peaks are expected at $\omega_1 = 2\pi\nu(H^\alpha)$ and $\omega_1 = 2\pi\nu(H^{\alpha'})$. However, in the experiment with decoupling during t_1 (see Figure 1 and 2), additional cross-peaks are found at $\omega_1 = 2\pi(\nu(H^\alpha) + \nu(H^{\alpha'}))/2$. These artifacts result from (band-selective) homonuclear TOCSY transfer between H^α and $H^{\alpha'}$ during the band-selective refocusing pulses that are applied at $t_1/2$ to the H^α and $H^{\alpha'}$ spins (Glaser and Quant, 1996).

For two spins, I_1 and I_2, (corresponding to H^α and $H^{\alpha'}$) with resonance frequencies in the active bandwidth of the band-selective inversion pulse, the pulse sandwich Gauss(90°_x) 180°_{-x} Gauss(90°_x) creates an effective Hamiltonian of the form

$$\mathcal{H}_{\text{eff}} \approx 2\pi J_{\text{eff}}(I_{1x}I_{2x} + I_{1y}I_{2y} + I_{1z}I_{2z}), \tag{A1}$$

with J_{eff} of about -15 Hz which results in efficient TOCSY transfer. Note that the H^N spins are decoupled from H^α and $H^{\alpha'}$ due to the selective inversion of the H^α and $H^{\alpha'}$ spins. In our experiments, the bandwidth of the Gaussian pulses was about 1.4 kHz. E.g., for glycine G57 (see Figure 2), the H^α and $H^{\alpha'}$ spins have offsets of $\nu(H^\alpha) = 376.6$ Hz and $\nu(H^{\alpha'}) = 451.6$ Hz, respectively. The numerically calculated effective Hamiltonian (Glaser and Drobny, 1990) created by the band-selective inversion sandwich of duration $\tau = 2\tau_{\text{Gauss}} + \tau_{180^\circ} = 9.112$ ms is given by

$$\begin{aligned}\mathcal{H}_{\text{eff}}(\text{G57}) = \; & 2\pi(7.3I_{1x} + 2.8I_{1y} - 1.1I_{1z} \\ & +6.4I_{2x} + 4.2I_{2y} - 2.2I_{2z} \\ & -14.2I_{1x}I_{2x} - 14.5I_{1y}I_{2y} - 14.4I_{1z}I_{2z} \\ & -1.4I_{1x}I_{2y} + 1.7I_{1y}I_{2x} - 2.7I_{1x}I_{2z} \\ & +2.6I_{1z}I_{2x} - 1.2I_{1y}I_{2z} + 1.4I_{1z}I_{2y})\tfrac{1}{s}.\end{aligned} \tag{A2}$$

For $\alpha, \beta, \gamma = \{x, y, z\}$ or cyclic permutations thereof, density operator terms $I_{1\alpha}$ evolve under the effective isotropic mixing Hamiltonian of Equation A1 as

$$I_{1\alpha} \rightarrow I_{1\alpha}\cos^2(\pi Jt) + (2I_{1\beta}I_{2\gamma} - 2I_{1\gamma}I_{2\beta})\sin(\pi Jt)\cos(\pi Jt) + I_{2\alpha}\sin^2(\pi Jt)$$

(Glaser and Quant, 1996) during the time τ of the pulse sandwich. Similarly, bilinear density operator terms evolve as

$$2I_{1\beta}I_{2\gamma} \rightarrow 2I_{1\beta}I_{2\gamma}\cos^2(\pi Jt) + (I_{2\alpha} - I_{1\alpha})\sin(\pi Jt)\cos(\pi Jt) + 2I_{1\gamma}I_{2\beta}\sin^2(\pi Jt)$$

and

$$2I_{1\alpha}I_{2\gamma} \rightarrow 2I_{1\alpha}I_{2\gamma}\cos^2(\pi Jt) - (I_{2\beta} - I_{1\beta})\sin(\pi Jt)\cos(\pi Jt) + 2I_{1\gamma}I_{2\alpha}\sin^2(\pi Jt).$$

For an initial density operator $\rho(0) = I_{1x} + I_{2x}$, the expectation value $\langle I_{1x} + I_{2x}\rangle$ as a function of t_1 is given by

$$\begin{aligned}\langle I_{1x} + I_{2x}\rangle(t_1) = \; & \cos(2\pi\nu_1 t_1)\{A\cos(\pi Jt_1) - B\sin(\pi Jt_1)\} \\ & +\cos(2\pi\nu_2 t_1)\{A\cos(\pi Jt_1) - B\sin(\pi Jt_1)\} \\ & +\cos(2\pi\bar{\nu}t_1)\{2C\cos(\pi Jt_1) + 2B\sin(\pi Jt_1)\}\end{aligned}$$

with

$$\begin{aligned}A &= \cos^2(\pi J\tau), \\ B &= \cos(\pi J\tau)\sin(\pi J\tau), \\ C &= \sin^2(\pi J\tau),\end{aligned}$$

and

$$\bar{\nu} = \frac{\nu_1 + \nu_2}{2}.$$

After Fourier transformation in t_1 dimension, we find the expected signals of spin I_1 (corresponding to H^α) at the frequency ν_1 and the expected signal of spin I_2 (corresponding to $H^{\alpha'}$) at the frequency ν_2. Each of these signals consists of an absorptive in-phase doublet with amplitude A and a dispersive anti-phase doublet with amplitude -B.

In addition, we find a signal at the average frequency $\bar{\nu} = (\nu_1 + \nu_2)/2$ which consists of an absorptive in-phase doublet with amplitude $2C$ and a dispersive anti-phase doublet with amplitude $2B$. E.g., for $J = -15$ Hz and $\tau = 9.112$ ms, these amplitudes are $A = 0.83$, $B = -0.38$, and $C = 0.17$.

Based on the effective Hamiltonian of Equation A2 (Glaser and Drobny, 1990) we numerically simulated ω_1-spectra for the spin system of G57. The corresponding experimental and simulated ω_1-spectra are shown in Figure 5 at the H^N frequency of G57. A reasonable match is found between theory and experiment. This analysis shows that one possible approach to reduce the artifacts in ω_1-decoupled spectra is to minimize the duration of the spin-selective inversion element.

References

Annila, A., Aitio, H., Thulin, E. and Drakenberg, T. (1999) *J. Biomol. NMR*, **14**, 223–230.

Aue, W.P., Bartholdi, E. and Ernst, R.R. (1976) *J. Chem. Phys.*, **64**, 2229–2246.

Bastiaan, E.W., MacLean, C., van Zijl, P.C.M. and Bothner-By, A.A. (1987) *Annu. Rep. NMR Spectrosc.,* **19**, 35–77.

Bax, A., Kontaxis, G. and Tjandra, N. (2001) *Meth. Enzymol.*, **339**, 127–174.

Bolon, P.J. and Prestegard, J.H. (1998) *J. Am. Chem. Soc.*, **120**, 9366–9367.

Brunner, E. (2001) *Concepts Magn. Reson.*, **13**, 238–259.

Brunner, E., Ogle, J., Wenzler, M. and Kalbitzer, H.R. (2000) *Biochem. Biophys. Res. Commun.*, **272**, 694–698.

Cai, M., Wang, H., Olejniczak, E.T., Meadows, R.P., Gunasekera, A.H., Xu, N. and Fesik, S.W. (1999) *J. Magn. Reson.*, **139**, 451–453.

Clore, G.M., Starich, M.R., Bewley, C.A., Cai, M. and Kuszewski, J. (1999) *J. Am. Chem. Soc.*, **121**, 6513–6514.

Cornilescu, G., Marquardt, J.L., Ottiger, M. and Bax, A. (1998) *J. Am. Chem. Soc.*, **120**, 6836–6837.

Delaglio, F., Kontaxis, G. and Bax, A. (2000) *J. Am. Chem. Soc.*, **122**, 2142–2143.

Delaglio, F., Wu, Z. and Bax, A. (2001) *J. Magn. Reson.*, **149**, 276–281.

Emsley, L. and Bodenhausen, G. (1992) *J. Magn. Reson.*, **97**, 135–148.

Fowler, C.A., Tian, F., Al-Hashimi, H.M. and Prestegard, J.H. (2000) *J. Mol. Biol.*, **304**, 447–460.

Glaser, S.J. and Drobny, G.P. (1990) In *Advances in Magnetic and Optical Resonance*, Vol. 14, Warren, W.S., ed., Academic Press, San Diego, pp. 35–58.

Glaser, S.J. and Quant, J.J. (1996) In *Advances in Magnetic and Optical Resonance*, Vol. 19, Warren, W.S. (Ed.), Academic Press, San Diego, pp. 59–252.

Griesinger, C., Søerensen, O.W. and Ernst, R.R. (1985) *J. Am. Chem. Soc.*, **107**, 6394–6396.

Gullion, T., Baker, D.B. and Conradi, M.S. (1990) *J. Magn. Reson.*, **89**, 479–484.

Hansen, M.R., Mueller, L. and Pardi, A. (1998a) *Nat. Struc. Biol.*, **5**, 1065–1074.

Hansen, M.R., Rance, M. and Pardi, A. (1998b) *J. Am. Chem. Soc.*, **120**, 11210–11211.

Jeener, J. (1971) AMPERE Summer School, Basko Polje, Yugoslavia.

Karplus, M. (1959) *J. Chem. Phys.*, **30**, 11–15.

Kay, L.E., Torchia, D.A. and Bax, A. (1989) *Biochemistry*, **28**, 8972–8979.

Kramer, F., Peti, W., Griesinger, C. and Glaser, S.J. (2001) *J. Magn. Reson.*, **149**, 58–66.

Lizak, M.J., Gullion, T. and Conradi, M.S. (1991) *J. Magn. Reson.*, **91**, 254–260.

Losonczi, J.A. and Prestegard, J.H. (1998) *J. Biomol. NMR*, **12**, 447–451.

Losonczi, J.A., Andrec, M., Fischer, M.W.F. and Prestegard, J.H. (1999) *J. Magn. Reson.*, **138**, 334–342.

Marion, D. and Wüthrich, K. (1983) *Biochem. Biophys. Res. Commun.*, **113**, 967–974.

Meiler, J., Peti, W. and Griesinger, C. (2000) *J. Biomol. NMR*, **17**, 283–294.

Mueller, G.A., Choy, W.Y., Yang, D., Forman-Kay, J.D., Venters, R.A. and Kay, L.E. (2000) *J. Mol. Biol.*, **300**, 197–212.

Ottiger, M. and Bax, A. (1998) *J. Biomol. NMR*, **12**, 361–372.

Otting, G., Rückert, M., Levitt, M.H. and Moshref A. (2000) *J. Biomol. NMR*, **16**, 343–346.

Pardi, A., Billeter, M. and Wüthrich, K. (1984) *J. Mol. Biol.*, **180**, 741–751.

Peti, W. and Griesinger, C. (2000) *J. Am. Chem. Soc.*, **122**, 3975–3976.

Prasch, T., Gröschke, P. and Glaser, S.J. (1998) *Angew. Chem. Int. Ed.*, **37**, 802–806.

Simon, B. and Sattler M. (2002) *Angew. Chem. Int. Ed.*, **41**, 437–440.

Tian, F., Fowler, C.A., Zartler, E.R., Jenney, Jr., F.A., Adams, M.W. and Prestegard, J.H. (2000) *J. Biomol. NMR*, **18**, 23–31.

Titman, J.J. and Keeler, J. (1990) *J. Magn. Reson.*, **89**, 640–646.

Tjandra, N. and Bax, A. (1997) *Science*, **278**, 1111–1114.

Vuister, G.W. and Bax, A. (1993) *J. Am. Chem. Soc.*, **115**, 7772–7777.

Willker, W. and Leibfritz, D. (1992) *J. Magn. Reson.*, **99**, 421–425.

Wlodawer, A., Nachman, J., Gilliland, G.L., Gallagher, W. and Woodward, C. (1987) *J. Mol. Biol.*, **198**, 469–480.